A Numerical Study of Nocturnal Sea Breezes: Prefrontal Gravity Waves in the Compensating Flow and Inland Penetration of the Sea-Breeze Cutoff Vortex

WEIMING SHA

Institute of Computational Fluid Dynamics, Meguro-Ku, Tokyo, Japan

TAKESHI KAWAMURA

Institute of Geoscience, University of Tsukuba, Ibaraki, Japan

HIROMASA UEDA

Research Institute for Applied Mechanics, Kyushu University, Kasuga, Fukuoka, Japan

(Manuscript received 29 April 1991, in final form 22 April 1992)

ABSTRACT

It is demonstrated in this numerical study that prefrontal perturbations may be triggered by a penetrating sea-breeze head into an existing nocturnal temperature inversion. The perturbations consist of the lower-layer wavelike perturbation and the upper-wave motion, both of which are manifested as rotor streaming. However, these prefrontal gravity waves take the form of the weak transient waves of a depression trapped in the ambient compensating flow field.

The sea-breeze head dissipates as it penetrates inland into the nocturnal temperature inversion. At midnight, a horizontal vortex is completely detached from the feeder flow of the sea breeze. This isolated horizontal vortex is identified as the sea-breeze cutoff vortex. It is shown that the sea-breeze cutoff vortex may be evolved from a dissipating sea-breeze head. After the sea-breeze cutoff vortex is formed, it propagates farther inland as an isolated wave-type disturbance. Examination of the force balance suggests that the inertia and radiative energy loss are dominant in the processes of the sea-breeze cutoff vortex.

1. Introduction

In a previous paper (Sha et al. 1991, hereafter SKU), the finestructure and dynamics of the sea-breeze head were investigated using a two-dimensional nonhydrostatic numerical model with high spatial resolution and an appropriate turbulence model. The distinctive turbulent structures associated with a street of horizontal vortices in the sea-breeze head could be simulated and these horizontal vortices were manifested as Kelvin–Helmholtz (KH) billows resulting from the Kelvin–Helmholtz instability (KHI). The KHI was found to occur in the foremost part of the sea-breeze head. Consequently, the KH billows were generated there and then grew in amplitude while traveling backward, relative to the advancing front of the sea breeze. The street of KH billows entrained the upper air into the sea breeze, and the resultant turbulent mixing and wave perturbation induced a top friction force acting on the sea-breeze head. Moreover, the inland penetration of the sea-breeze head was found to be retarded when KHI occurred and the induced top friction force acted on the sea-breeze head. It was also shown that the KHI did not occur at all stages of the sea breeze, and the fine structure and dynamics of the head in different stages were significantly different.

General features of the sea breeze in coastal areas are as follows: after sunset, the land surface begins to cool due to longwave radiation and the adjacent air layer becomes stably stratified. The sea-breeze front, however, continues to move inland, so that the penetrating sea-breeze front impinges upon the developing temperature inversion ahead of it. As mentioned briefly in SKU, as a result of the impingment of the sea-breeze head onto the nocturnal inversion, prefrontal perturbations are generated ahead of the penetrating sea-breeze front. At about 2400 LST, the foremost part of the sea breeze begins to separate from the feeder flow, and then, for some time later, the sea-breeze cutoff vortex is evolved from the dissipating sea-breeze head and propagates farther inland.

From early observations in the midwestern United States Tepper (1950) speculated that a bore was produced by the impulsive motion of a cold front into an existing nocturnal inversion. The mechanism Tepper

Corresponding author address: Dr. Weiming Sha, Institute of Computational Fluid Dynamics, 1-22-3, Haramachi, Meguro-ku, Tokyo, 152 Japan.

used in generating the bores in the atmosphere finds support in several laboratory experiments using density-stratified fluids (Maxworthy 1980; Simpson 1982; Smith et al. 1982; Wood and Simpson 1984; Rottman and Simpson 1989). These laboratory experiments have demonstrated that a gravity current moving into a stratified fluid can produce undular bores ahead of it. Obviously, the common feature of the proposed generation mechanisms for internal bores or internal gravity waves in the atmosphere is that they are the result of interaction between a gravity current and the existing temperature inversion. Therefore, any kind of atmospheric gravity current, such as deeply penetrating sea-breeze heads, thunderstorm outflows, katabatic flows and cold fronts, that moves into an existing inversion waveguide can be expected to generate internal bores or internal gravity waves.

A variety of atmospheric phenomena have been interpreted as the result of internal bores or internal solitary waves propagating in the low-level temperature inversion. One of the most interesting and best documented examples of atmospheric bores is the so-called "morning glory" phenomenon in Australia. Clarke (1972) and Clarke et al. (1981) hypothesized that the northeasterly morning glory is produced by the interaction of a sea-breeze front or katabatic wind with a nocturnal or maritime inversion. Later, Clarke (1984) and Noonan and Smith (1986, 1987) showed in their numerical simulations that even in the collision of two opposing sea-breeze fronts in the Gulf of Carpentaria and Cape York Peninsula region of northeastern Australia, an internal bore arose in the lower atmosphere. As for the southerly morning glory, Smith et al. (1982) proposed that it is produced by a mesoscale front interacting with an existing temperature inversion. In a number of studies carried out in recent years (Christie et al. 1981; Christie and Muirhead 1983; Clarke 1983; Smith and Morton 1984; Drake 1985; Smith et al. 1986; Physick 1986), there is increasing evidence that the morning glory is, in essence, a long nonlinear internal boundary-layer wave disturbance. Other similar types of disturbances have also been observed in many parts of the world (Shreffler and Binkowski 1981; Hasse and Smith 1984; Doviak and Ge 1984; Fulton et al. 1990; Cheung and Little 1990; Doviak et al. 1991). Observations of solitary wave and borelike disturbances in the lower atmosphere are reviewed recently by Smith (1988).

Theoretical works on internal bores and solitary waves in the surface-based stable layer have been reviewed by Christie et al. (1978, 1979) and Noonan and Smith (1985) and more recently by Christie (1989). In the deep-fluid case, evolution of a boundary-layer disturbance with modest amplitude is governed by the so-called Benjamin–Davis–Ono (BDO) equation (Benjamin 1967; Davis and Acrivos 1967; Ono 1975). Detailed comparisons were made by Noonan and Smith (1985) between the BDO theory and the observed morning glory–type disturbances in the lower atmosphere. However, the result was not so satisfactory. At the present time, the long weakly nonlinear wave theory is still quantitatively unreliable for large amplitude waves that have a recirculating region (Tung et al. 1982; Christie 1989; Doviak et al. 1991).

That a gravity current moving into a stably stratified fluid can generate an undular bore is well known from the numerical simulations of Crook and Miller (1985), Crook (1986, 1988), and Haase and Smith (1989). In the real atmosphere, however, any atmospheric gravity current and the surrounding ambient environment are substantially unsteady. The land/sea breeze is typical. For example, when the head of a sea breeze penetrates into a nocturnal temperature inversion during nighttime, not only is the temperature inversion is stabilizing in time, but the sea-breeze head is dissipating. So, it is necessary in a numerical simulation to fully examine the evolution and structure of the sea-breeze head and its triggering phenomena. An attempt is made in this numerical study to model the full-time dependent behavior of the sea-breeze head and the interaction of this head with a nocturnal temperature inversion after sunset.

The internal bore or internal gravity wave is damped through upward radiation of wave energy if the fluid layer above the waveguide is stratified stably, and the damping mechanism is significantly affected by the stratification (Maslowe and Redekopp 1980; Grimshaw 1981a,b). In general, an internal bore propagating some distance horizontally in front of a gravity current transmits its energy to vertically propagating gravity waves in the upper layer of a continuously stratified fluid, and the amplitude and duration of the disturbance are limited. In two recent papers Crook (1986, 1988) suggested that when a bore propagates any significant distance, the following mechanisms could trap the vertically propagating waves: 1) upper-level opposing winds; 2) lower-level opposing winds, and 3) an inversion at some height in the upper layer. He demonstrated further that whenever an atmospheric bore propagated a significant distance, at least one, and sometimes all three, of these trapping mechanisms took place—of which the lower-level opposing flow was the most prevalent mechanism for trapping energy at low levels.

The transformation of a gravity current into an isolated-type wave has been described by Haase and Smith (1989) and Haase (1991). Simpson et al. (1977) made a detailed field observation of the sea breeze in southern England and showed that although the sea-breeze front in early afternoon had been of the normal gravity current form, by late afternoon the foremost part of the sea breeze was separated from the feeder flow. Following Clarke (1965), they called this separated part of the sea breeze a sea-breeze vortex and suggested that the deeply penetrating sea-breeze front is mostly in the form of such a cutoff vortex. In this numerical exper-

iment, we will demonstrate the possibility for a sea-breeze cutoff vortex (defined in section 3b) to evolve from the dissipating sea-breeze head at midnight.

Also investigated are the evolution and structures of the prefrontal gravity waves and sea-breeze cutoff vortex using a numerical model. In section 2 a brief description of the numerical model is made. Section 3 contains numerical results and discussion. The evolution and structures of the prefrontal gravity waves and sea-breeze cutoff vortex are examined, respectively. Conclusions and an outlook on further work are presented in section 4.

2. Numerical model

The numerical model employed in this study was the same as in SKU. Only a brief description of the model features will be given here.

The model was based on a set of two-dimensional, nonhydrostatic, primitive equations for a compressible, dry-adiabatic fluid. The eddy diffusivity was evaluated from the $E - \epsilon$ turbulence model.

The numerical calculation was performed on a domain of 226 km $\times$ 5.4 km in the x, z directions, respectively. The grid number was 690 $\times$ 49 and the time increment was 30 s. A staggered grid scheme was constructed and the differential equations were discretized using the control volume method with fully implicit formulation for the time derivatives.

Initial conditions were specified as no ambient motion and a constant temperature lapse rate. These represent synoptic conditions for a clear and calm day dominated by a high pressure system, with no geostrophic wind. At the bottom, the no-slip condition was imposed. The sea surface temperature was kept constant and the land temperature was given as a sinusoidal function of time. Rates of momentum and heat transfer at the earth's surface were evaluated from the so-called shear functions. At the lateral boundaries, the radiation condition was used to compute the boundary values of velocity components, u and v, while the vertical velocity w at the lateral boundary was calculated to satisfy mass conservation. The scalar variables were calculated at the lateral boundaries based on the assumption that their derivatives with respect to x are equal to zero. At the top boundary, all variables were fixed at their initial values. The time integration was initiated at 0800 LST Day 1 and continued for 48 h while the numerical results were regarded as a good representation of a diurnally varying atmosphere.

3. Results and discussions

a. *Evolution and structures of prefrontal gravity waves*

Figure 1 shows the hourly evolution of the sea-breeze head and prefrontal gravity waves from 2100 to 2400 LST. At 2100 (all times local hereafter), the temperature inversion over land has been formed through the longwave radiative cooling and still continues to intensify with time. However, the nocturnal radiation inversion is shallow. Above it, a layer of weak or almost neutral stratification up to 800 m, caused by the thermal convective mixing over the land at daytime, exists and changes little afterward. As can be seen in Fig. 1, at 2100 a closed circulation remains in the penetrating sea-breeze head, and then the sea-breeze front is impinging the existing temperature inversion as it advances inland. Its advance speed is almost constant, that is, 5.9 km h^{-1} during this time period (see in SKU, Fig. 12). Ahead of the front, perturbations appear. They are considered to be triggered by the advancing sea-breeze head; that is, the head acts as an initiator of these perturbations, and energy is believed to be supplied from the penetrating head to the perturbations. Actually, these prefrontal perturbations appeared in early evening when the thermal convective activity ceased. In the frontal region of the sea breeze, a strong updraft exists. To compensate for this, an opposing flow is created directed toward the front from the land side in the lowermost layer. Thus, a return flow is created in the upper layer, and a wind shear is built up in these layers. In both lowermost and upper layers, wavelike perturbations appear that are manifested as rotor streaming. The representative wavelength in the upper layer is about 10 km, and the propagation speed is 12.6 km h^{-1}.

However, these prefrontal perturbations are essentially weak because an examination of the relative streamline pattern shows that the relative flow in Fig. 1 is through the prefrontal disturbance at all levels. These prefrontal perturbations take the form of weak transient waves of depression trapped in the ambient compensating flow field that develops ahead of the advancing sea-breeze front during early evening. The structures and properties are different from the known bores or morning glory waves. The weak disturbances of this type may not as yet have been observed because of their small amplitude.

The sea-breeze head is dissipating as it moves inland during late evening. At 0000, the leading part of the sea-breeze head begins to separate from the feeder flow, and the prefrontal gravity waves become a large-scale wave motion and seem to no longer have sufficient energy supply from the dissipating head to maintain themselves.

In the continuously stably stratified atmosphere, internal bores or internal gravity waves are to be created by the sea-breeze head, thunderstorm outflow, cold front, and so on. However, if the stratified upper layer allows the energy of disturbances to be radiated upward, the amplitude and lifetime of these disturbances are limited. The prefrontal gravity waves in this numerical simulation decay with time and the lifetime is about 3 h. Here, it is interesting to investigate the waveguide structures on which these weak gravity waves propagate

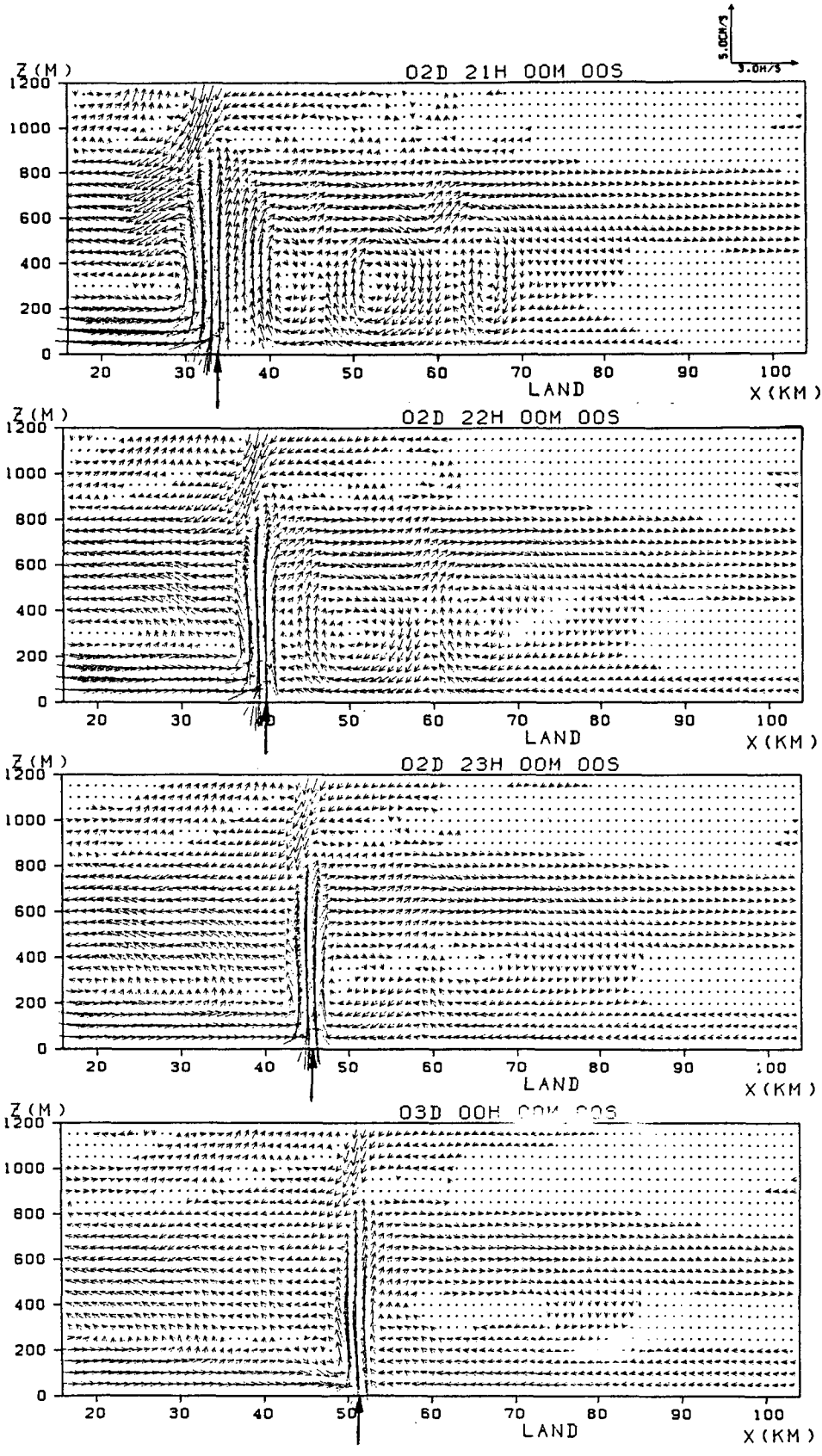

FIG. 1. Vertical cross sections of wind vectors for a successive time series at 2100, 2200, 2300, 2400 LST. Dots represent the points where the horizontal velocity u is less than 0.1 m s^{-1} while the vertical velocity w is less than 0.1 cm s^{-1}. The numbers on the horizontal axis denote distance from the coastline. The arrows indicate the location of sea-breeze front at each time.

after they are produced ahead of the penetrating front and, accordingly, to elucidate the full time-dependent development of these gravity waves. The upward energy radiation has been examined theoretically by Scorer (1949) for the gravity waves in the flow over mountains. He showed that energy can be trapped at low levels when the parameter (commonly called the Scorer parameter)

$$l^2 = \frac{g}{(u-c)^2}\frac{1}{\theta}\frac{\partial\theta}{\partial z} - \frac{1}{u-c}\frac{\partial^2 u}{\partial z^2} \qquad (1)$$

decreases with height; c is the penetration speed of the waves. As can be seen, the Scorer parameter l^2 is determined by the ambient static stability and the ambient horizontal wind profile. To explain the amplitude and lifetime of the observed gravity wave disturbances, Crook proposed three wave-trapping mechanisms based upon the numerical studies (Crook 1986, 1988). The first mechanism occurs when winds in the upper layer oppose the wave motion. This reduces the Scorer parameter in the upper layer and leads to wave evanescence in that region. The second mechanism occurs when a jet exists in the lower layer that opposes the wave motion. It is shown that the curvature in the velocity profile above this jet can produce a layer of negative Scorer parameter, and a considerable amount of energy can be trapped below the layer. The third mechanism occurs when an inversion exists at a certain height above the lower stable layer. The inversion reflects the upward energy radiation and leads to an enhancement of the wave amplitude in the lower layer. Figure 2 shows the profiles of horizontal velocity u, potential temperature θ, vertical velocity w, and calculated Scorer parameter l^2 at $x = 60$ km, just downwind of the prefrontal gravity waves at 2200. It is seen in Fig. 2a that the flow in the lower layer (below 450 m) opposes the motion of the sea-breeze front, while in the layer between 450 m and 1050 m, it is in the same direction as the wave motion. As already depicted in Fig. 1, a strong updraft exists in the leading part of the sea-breeze head, and the opposite low-level flow arises to compensate for the large horizontal convergence at the frontal region. Figure 2b shows that the prefrontal gravity waves propagate in a layer of weak or almost neutral stratification, bounded by a shallow surface inversion layer and a stably stratified layer above 800 m. The value of the Scorer parameter l^2 is plotted in Fig. 2d. Also plotted are the wind curvature term

$$-\frac{1}{u-c}\frac{\partial^2 u}{\partial z^2}$$

and the static stability term

$$\frac{g}{(u-c)^2}\frac{1}{\theta}\frac{\partial\theta}{\partial z}$$

in (1). As can be seen, the static stability term decreases with height in the lower layer and then increases. The curvature term decreases with height and reaches its minimum at the top of the opposite low-level flow. The Scorer parameter is large and positive in the lowermost layer because of the strong surface inversion. It decreases with height and upon changing sign attains a minimum at the top of the opposite flow layer. A layer with a negative Scorer parameter is created; thus, a substantial amount of energy is trapped inside the lower layer, while the layer above it, in which the Scorer parameter increases drastically with height and has a large positive value, allows energy to be radiated upward. Therefore, it may be concluded that the wave perturbation propagates in the lower layer where the Scorer parameter decreases with height and the upward energy radiation is prohibited while the wave motion in the upper layer dissipates its energy quickly due to the upward energy radiation.

The Richardson number Ri, calculated from

$$\mathrm{Ri} = \frac{g}{\theta}\frac{\partial\theta}{\partial z}\Big/\left(\frac{\partial u}{\partial z}\right)^2 \qquad (2)$$

is presented in Fig. 3. At all levels, Ri is much larger than the critical value (Ri = 0.25) for the Kelvin–Helmholtz instability (KHI). Therefore, it is considered that such a instability does not occur through the layer examined here.

At midnight (0000 LST), the apparent prefrontal disturbance has disappeared and a large-scale wave motion appears instead. Figure 4 shows the same profiles as in Fig. 2 but at 0000. At this stage, the Scorer parameter has a minimum at about the 100-m level. In the layer above it, it has a significant positive value to allow upward energy radiation.

In this way it could be argued from the numerical approach that prefrontal perturbations may be triggered in an existing nocturnal temperature inversion by the inland penetrating sea breeze. However, these prefrontal perturbations are weak waves of depression trapped in the ambient compensating flow field and do not appear to be comparable with the known bores or morning glory waves. It is confirmed that as the opposing flow exists in the lower layer, the curvature in the velocity profile at the top of this flow region contributes to produce a layer of negative Scorer parameter. Thus, a considerable amount of energy can be trapped below that layer, and the prefrontal gravity waves triggered by the penetrating front can be maintained. Of similar importance, a low-level jet required for the maintenance of long-lived squall lines has been argued by Thorpe et al. (1982), Rotunno et al. (1988), Weisman et al. (1988), Carbone et al. (1990), and Crook et al. (1990).

As there is no geostrophic wind in the present study, the low-level opposing wind is driven to compensate for the horizontal convergence in the frontal region of the penetrating sea-breeze head. When the head dis-

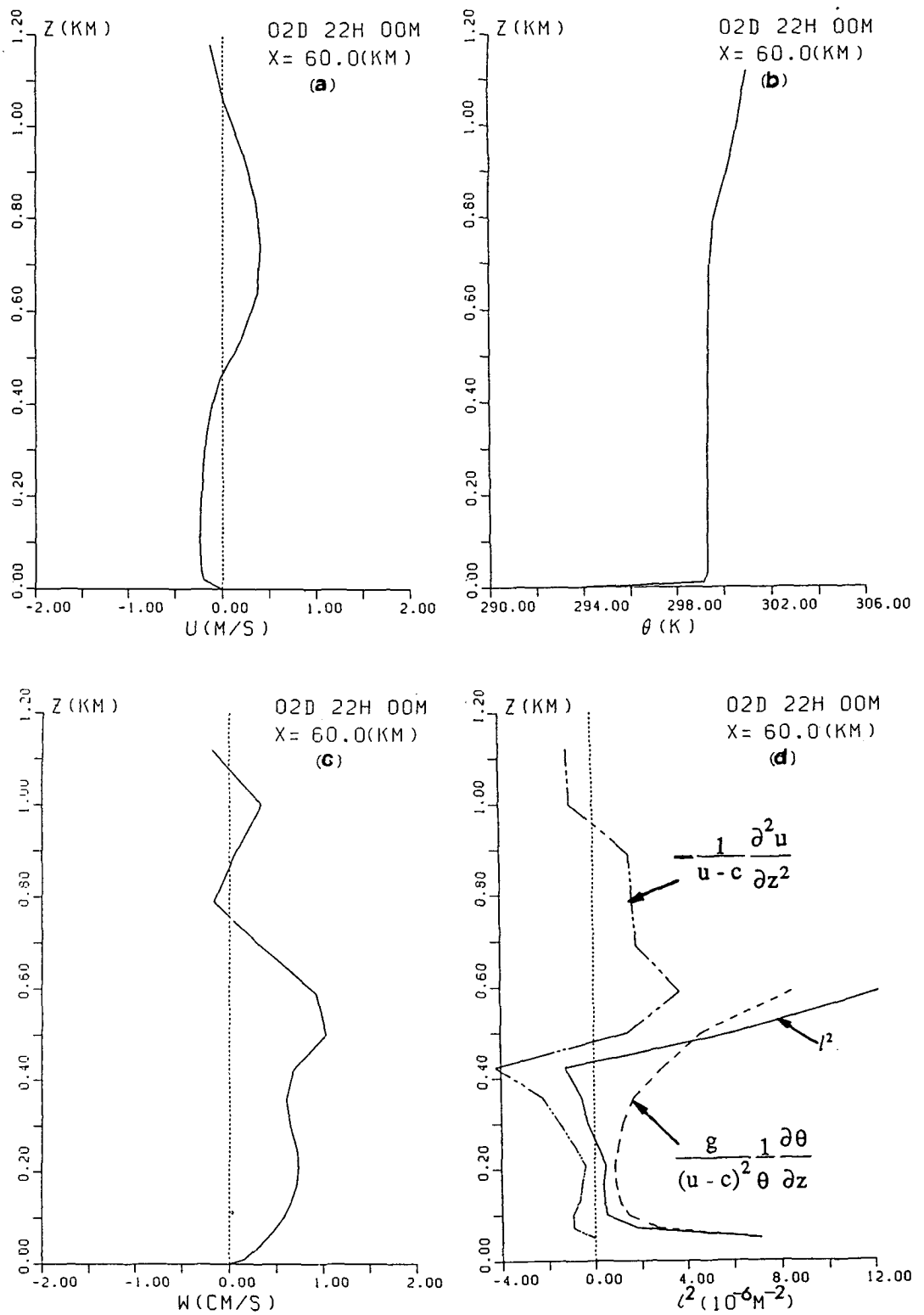

FIG. 2. Vertical profiles of (a) horizontal velocity, (b) potential temperature, (c) vertical velocity, (d) Scorer parameter vs height at $x = 60$ km, just downwind of the prefrontal gravity waves, at 2200 LST.

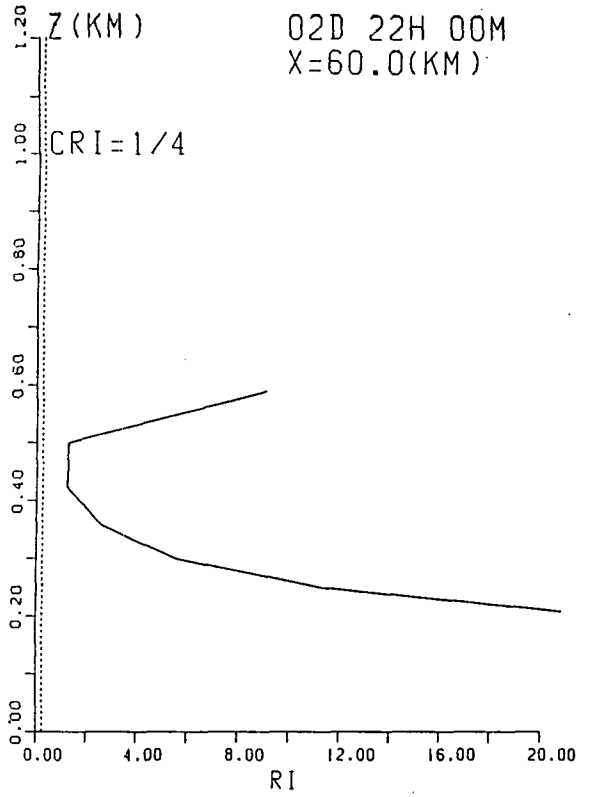

FIG. 3. As in Fig. 2 except for the Ri number.

sipates as it penetrates inland, the opposing low-level flow is also weakened. Moreover, the waveguide inversion in this numerical simulation is shallow. This may account for the failure to generate a significant prefrontal bore or solitary wave family. Consequently, it can be expected that prefrontal perturbations, triggered by a penetrating sea-breeze head on a waveguide with a suitable ambient condition, would be more powerful and long-lived. Investigation about the effects of ambient wind and stratification on these prefrontal perturbations is an important future task.

b. *Evolution and structure of the sea-breeze cutoff vortex*

As the sea-breeze head penetrates farther inland, it becomes more dissipated. By midnight the prefrontal gravity waves could not be sustained due to the upward energy radiation at the upper layer and the lack of energy supply from the dissipating head; they eventually disappeared. At the same time, the leading part of the sea-breeze head began to separate from the feeder flow. In this section, we will describe the spatial and temporal variations of the sea-breeze cutoff vortex and its structure.

Formation and evolution of the sea-breeze cutoff vortex are shown in Fig. 5. The leading part of the dissipating sea-breeze head continues to separate from the feeder flow, and then at 0100 a horizontal vortex is formed. The feeder flow of the sea breeze is shrunken. At 0200 a horizontal vortex is completely detached from the feeder flow and is established. We identify this kind of isolated horizontal vortex as a sea-breeze cutoff vortex. The sea-breeze cutoff vortex is steep in form, and its vertical motion is stronger in the frontal region than the rear. Here the sea-breeze cutoff vortex is different in shape and structure from the closed circulation that remains at the leading part of the deeply penetrating sea-breeze head and the rotor streaming motion (see in Fig. 1), and can be distinguished clearly. Also at this time, a component of the land breeze has appeared near the land surface in the region behind the sea-breeze cutoff vortex and advances toward the sea side. As time proceeds, the sea-breeze cutoff vortex, with its energy dissipating, propagates farther inland. Its average propagation speed is about 5.8 km h^{-1} (see in SKU, Fig. 12). Finally, the sea-breeze cutoff vortex disappears by dawn and the land breeze becomes prominent. The average length and mean height of the sea-breeze cutoff vortex, estimated from the zero streamline, are 20 km and 600 m, respectively. Since the sea-breeze cutoff vortex is able to advance farther inland with a closed circulation after it evolves from the dissipating sea-breeze head, it is thought that pollutants and humidity might be transported farther inland than by the original sea-breeze head.

To investigate the structure of the sea-breeze cutoff vortex, the vertical profiles of horizontal velocity u, potential temperature θ, and vertical velocity w across the sea-breeze cutoff vortex at 0200 are shown in Fig. 6. For comparison, the cross section of ambient environment (x = 73 km) is shown in Fig. 7, just ahead of the sea-breeze cutoff vortex. It is found that the arrival of the sea-breeze cutoff vortex is clearly marked by a squally wind in the lower layer. Nevertheless, since the change in the potential temperature profile is not so remarkable, the sea-breeze cutoff vortex is considered to move inland as an internal wave-type disturbance rather than a gravity current.

The vertical profile of Ri across the sea-breeze cutoff vortex (not shown) is of positive value much larger than the critical value for Kelvin–Helmholtz instability. Therefore, entrainment of the upper air by Kelvin–Helmholtz billows no longer occurs, as was seen in the active sea-breeze period, the details of which were investigated in SKU. Thus, the turbulent mixing at the top of the sea-breeze cutoff vortex is not significant. Examination of the forces acting on the sea-breeze cutoff vortex shows that the horizontal pressure gradient force is small because little temperature difference exists across it. The drag at the bottom of the sea-breeze cutoff vortex caused by surface friction is small and can be consistently neglected (see in SKU, Fig. 15). This is also so for the friction drag at the top of the sea-breeze cutoff vortex since turbulent mixing as in the active

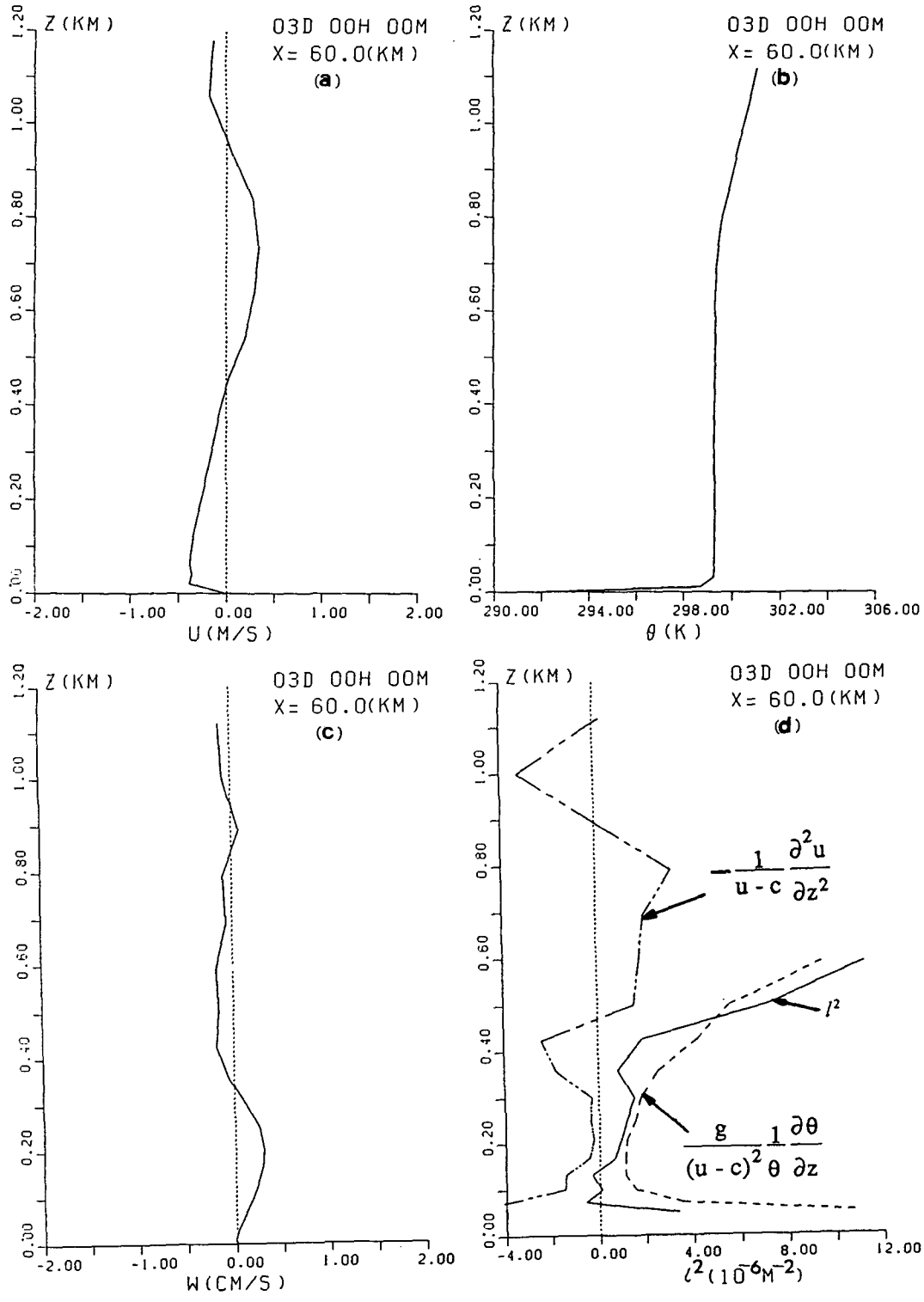

FIG. 4. As in Fig. 2 except for 0000 LST.

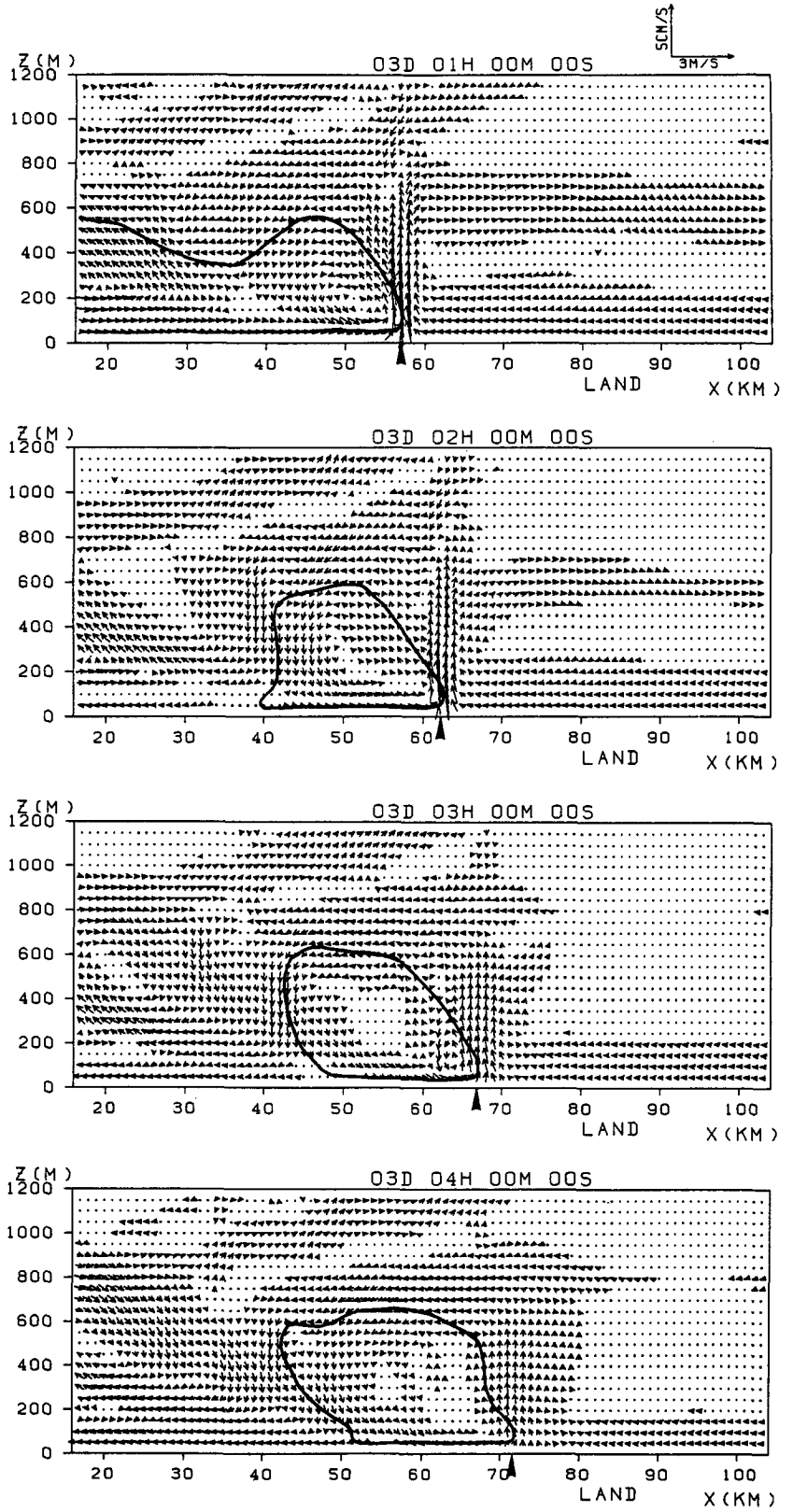

FIG. 5. As in Fig. 1 except for 0100, 0200, 0300, 0400 LST. The arrows indicate the frontal region of sea-breeze cutoff vortex. Solid line indicates zero streamline.

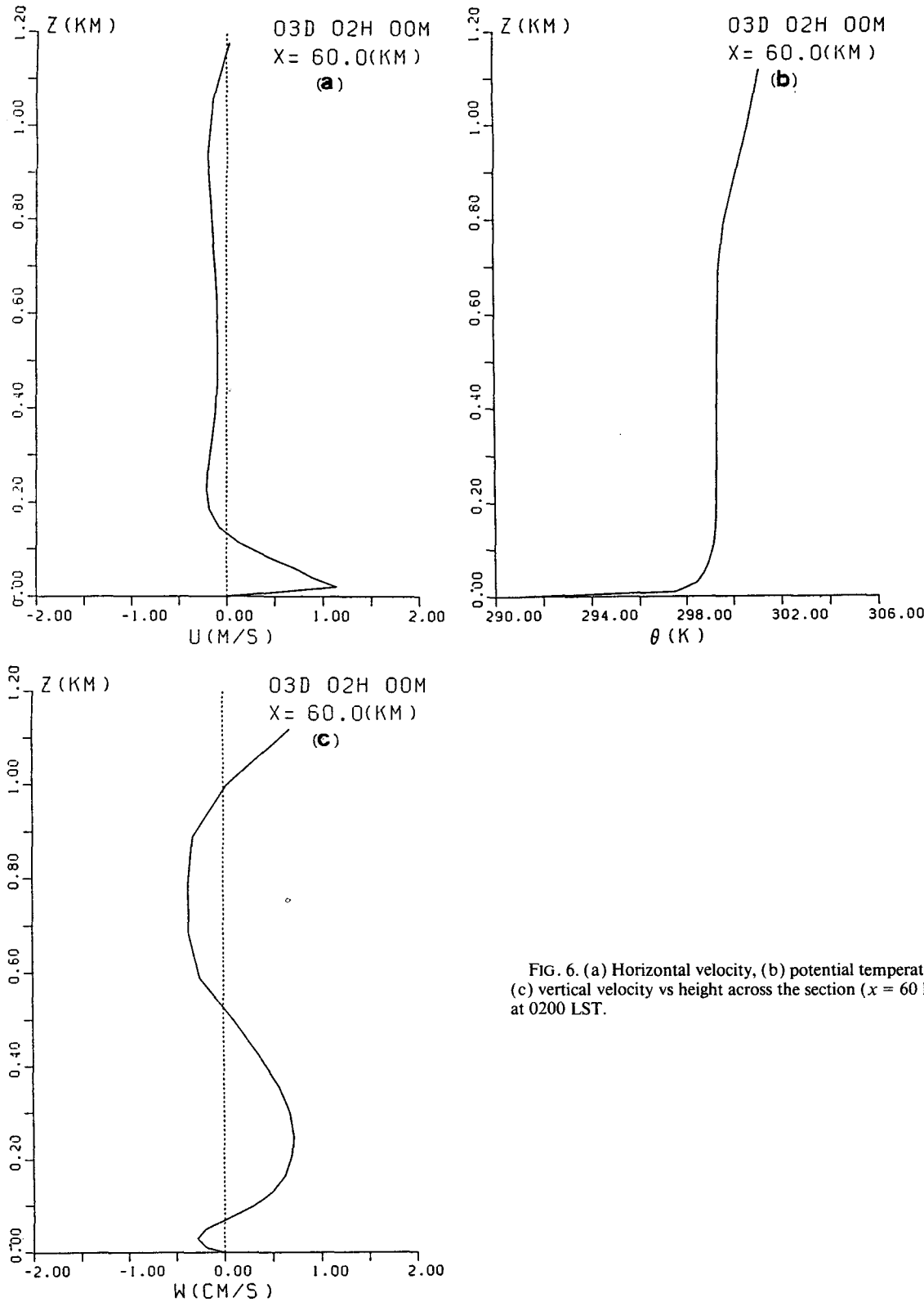

FIG. 6. (a) Horizontal velocity, (b) potential temperature, (c) vertical velocity vs height across the section (x = 60 km) at 0200 LST.

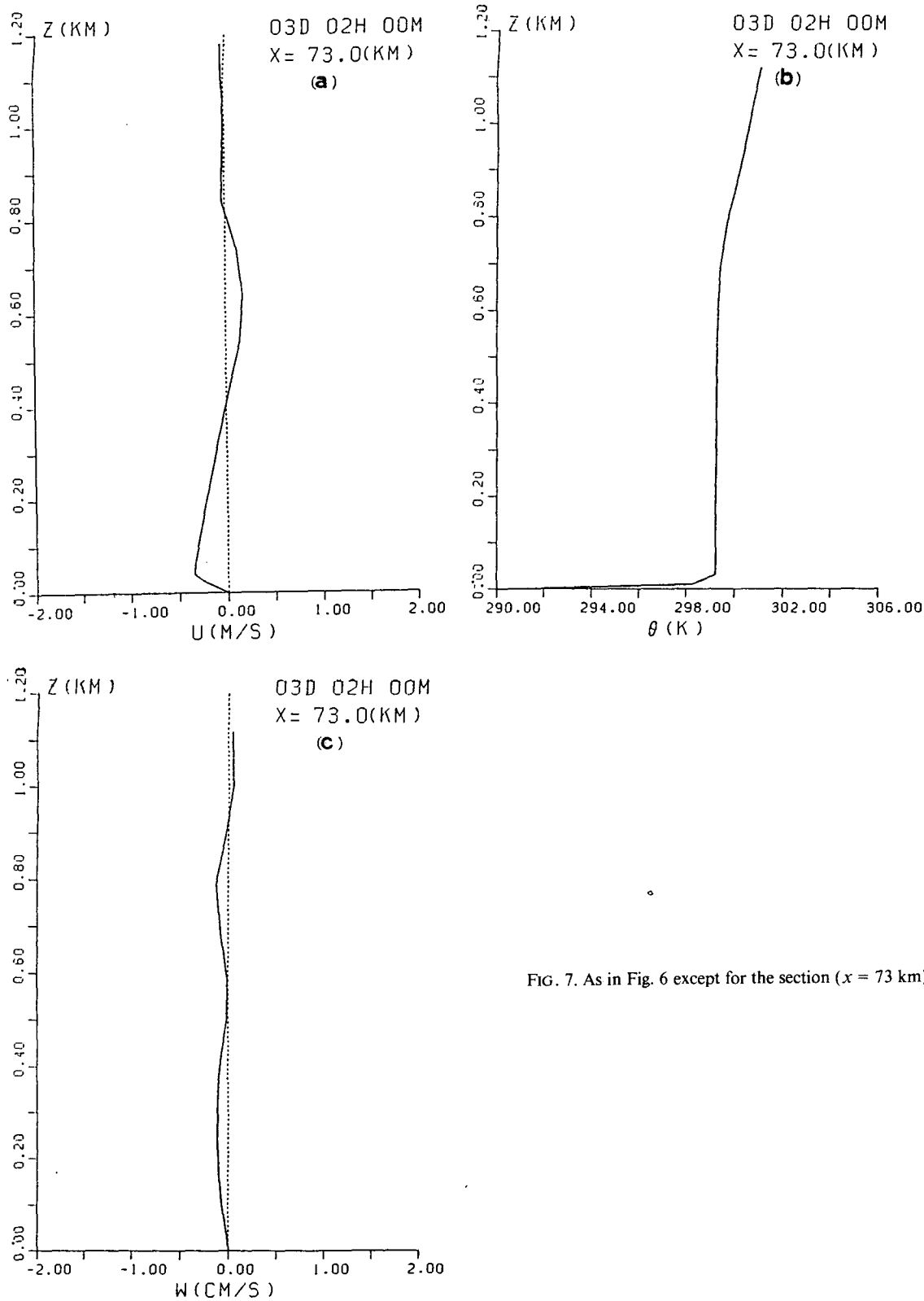

FIG. 7. As in Fig. 6 except for the section (x = 73 km).

sea-breeze period no longer occurs. Therefore, it may be concluded that the sea-breeze cutoff vortex is in such a state that inertia and radiative energy loss are dominant.

As might be supposed, the formation, evolution, and structure of the sea-breeze cutoff vortex are more complicated in the real atmosphere than in our numerical model; effects such as three dimensionality, wind shear, stratification in an ambient environment, topography, and the state of the earth's surface may be significant. The results in this numerical study, however, show that the sea-breeze cutoff vortex may evolve from a dissipating sea-breeze head under appropriate conditions and then move farther inland as an isolated wave-type disturbance.

4. Summary and outlook

In the course of investigating the land/sea breeze using a two-dimensional numerical model, special attention was focussed the sea-breeze behavior during late evening. It was demonstrated that prefrontal perturbations are triggered by a penetrating sea-breeze head in the nocturnal stable layer. The evolution and structure of these prefrontal gravity waves were minutely examined. They consisted of a lower-layer wavelike perturbation and an upper wave motion, both of which were manifested as rotor streaming. However, the structure and properties of these prefrontal perturbations were different from those of the known bores or morning glory waves. These prefrontal perturbations took the form of the weak transient waves of depression trapped in the ambient compensating flow field. The opposing low-level flow, driven to compensate for the horizontal convergence at the leading part of the sea-breeze head, was important in trapping upward radiative energy; it was confirmed to be one of the wave-trapping mechanisms suggested by Crook. After examining the profile of Ri, it was concluded that the Kelvin–Helmholtz instability did not occur in these prefrontal gravity waves.

The sea-breeze head dissipated as it advanced inland by late evening. At 0000 LST, the prefrontal gravity waves disappeared eventually, due to upward energy radiation in the waveguide layer and lack of an energy supply from the dissipating sea-breeze head. At this stage the leading part of the inland-penetrating sea-breeze head began to separate from the feeder flow. By 0200 LST, a horizontal vortex was completely detached from the feeder flow. This kind of isolated horizontal vortex was identified as the sea-breeze cutoff vortex. As time proceeded, the sea-breeze cutoff vortex propagated farther inland and finally disappeared by dawn.

The evolution and structure of the sea-breeze cutoff vortex were also investigated. It was found that after the sea-breeze cutoff vortex had formed, it propagated farther inland as an isolated wave-type disturbance. Examination of the force balance on the sea-breeze cutoff vortex suggested that the forces on the top and bottom surfaces and on the front and rear sides were not significant; so it was inferred that the inertia and radiative energy loss were dominant in the processes of the sea-breeze cutoff vortex.

The evolution and structure of prefrontal perturbations and the sea-breeze cutoff vortex phenomena, appearing as the sea-breeze front penetrates into an existing nocturnal inversion, are supposed to be more complicated in the real atmosphere; that is, effects such as the three-dimensionality, wind shear, and stratification in the ambient environment are significant and will be discussed in a subsequent paper.

Acknowledgments. We wish to express our appreciation to Dr. Douglas R. Christie of the Australian National University for his many fruitful comments on this manuscript. The research was partly supported by Grants-in-Aid for Scientific Research, No. 01155075 and No. 02201137, from the Ministry of Education, Science, and Culture, Japan.

REFERENCES

Benjamin, T. B., 1967: Internal waves of permanent form in fluids of great depth. *J. Fluid Mech.*, **29,** 559–592.

Carbone, R. E., J. W. Conway, N. A. Crook, and M. W. Moncrieff, 1990: The generation and propagation of a nocturnal squall line. Part I: Observations and implications for mesoscale predictability. *Mon. Wea. Rev.*, **118,** 26–49.

Cheung, T. K., and C. G. Little, 1990: Meteorological tower, microbarograph array, and sodar observations of solitary-like waves in the nocturnal boundary layer. *J. Atmos. Sci.*, **47,** 2516–2536.

Christie, D. R., 1989: Long nonlinear waves in the lower atmosphere. *J. Atmos. Sci.*, **46,** 1462–1491.

——, and K. J. Muirhead, 1983: Solitary waves: A hazard to aircraft operating at low altitudes. *Aust. Meteor. Mag.*, **31,** 97–109.

——, ——, and R. H. Clark, 1981: Solitary waves in the lower atmosphere. *Nature,* **293,** 46–49.

——, ——, and A. L. Hales, 1978: On solitary waves in the atmosphere. *J. Atmos. Sci.*, **35,** 805–825.

——, ——, and ——, 1979: Intrusive density flows in the lower troposphere: A source of atmospheric solitions. *J. Geophys. Res.*, **84,** 4959–4970.

Clarke, R. H., 1965: Horizontal mesoscale vortices in the atmosphere. *Aust. Meteor. Mag.*, **50,** 1–25.

——, 1972: The Morning Glory: An atmospheric hydraulic jump. *J. Appl. Meteor.*, **11,** 304–311.

——, 1983: Fair weather nocturnal inland wind surges and atmospheric bores. Part II: internal atmospheric bores in northern Australia. *Aust. Meteor. Mag.*, **31,** 147–160.

——, 1984: Colliding sea-breeze and the creation of internal atmospheric bore waves: Two-dimensional numerical studies. *Aust. Meteor. Mag.*, **32,** 207–226.

——, R. K. Smith, and D. G. Reid, 1981: The Morning Glory of the Gulf Carpentaria: An atmospheric undular bore. *Mon. Wea. Rev.*, **109,** 1726–1750.

Crook, N. A., 1986: The effect of ambient stratification and moisture on the motion of atmospheric undular bores. *J. Atmos. Sci.*, **43,** 171–181.

——, 1988: Trapping of low-level internal gravity waves. *J. Atmos. Sci.*, **45,** 1533–1541.

——, and M. J. Miller, 1985: A numerical and analytical study of atmospheric undular bores. *Quart. J. Roy. Meteor. Soc.*, **111,** 225–242.

——, R. E. Carbone, M. W. Moncrieff, and J. W. Conway, 1990:

The generation and propagation of a nocturnal squall line. Part II: Numerical simulations. *Mon. Wea. Rev.*, **118,** 50–65.

Davis, R. E., and A. Acrivos, 1967: Solitary internal waves in deep water. *J. Fluid Mech.*, **29,** 593–607.

Doviak, R. J., and R. S. Ge, 1984: An atmospheric solitary gust observed with a Doppler radar, a tall tower, and a surface network. *J. Atmos. Sci.*, **41,** 2559–2573.

——, S. S. Chen, and D. R. Christie, 1991: A thunderstorm-generated solitary wave observation compared with theory for nonlinear waves in a sheared atmosphere. *J. Atmos. Sci.*, **48,** 87–111.

Drake, V. A., 1985: Solitary wave disturbances of the nocturnal boundary layer revealed by radar observations of migrating insects. *Bound.-Layer Meteor.*, **31,** 269–286.

Fulton, R., D. S. Zrnić, and R. J. Doviak, 1990: Initiation of a solitary wave family in the demise of a nocturnal thunderstorm density current. *J. Atmos. Sci.*, **47,** 319–337.

Grimshaw, R., 1981a: Evolution equations for long, nonlinear internal waves in stratified shear flows. *Stud. Appl. Math.*, **65,** 159–188.

——, 1981b: Slowly varying solitary waves in deep fluids. *Proc. Roy. Soc. London,* **376A,** 319–332.

Haase, S. P., 1991: Numerical simulation of the bore-like cold front of 8 October 1987 in southern Germany. *Tellus,* **43A,** 97–105.

——, and R. K. Smith, 1984: Morning glory wave clouds in Oklahoma: A case study. *Mon. Wea. Rev.*, **112,** 2078–2089.

——, and ——, 1989: The numerical simulation of atmospheric gravity currents. Part II. Environments with stable layers. *Geophys. Astrophys. Fluid Dyn.*, **46,** 35–51.

Maslowe, S. A., and L. G. Redekopp, 1980: Long nonlinear waves in stratified shear flows. *J. Fluid Mech.*, **101,** 321–348.

Maxworthy, T., 1980: On the formation of nonlinear internal waves from the gravitational collapse of mixed regions in two and three dimensions. *J. Fluid Mech.*, **96,** 47–64.

Noonan, J. A., and R. K. Smith, 1985: Linear and weakly nonlinear internal wave theories applied to "Morning Glory" waves. *Geophys. Astrophys. Fluid Dyn.*, **33,** 123–143.

——, and ——, 1986: Sea-breeze circulations over Cape York Peninsula and the generation of Gulf of Carpentaria cloud-line disturbances. *J. Atmos. Sci.*, **43,** 1679–1693.

——, and ——, 1987: The generation of north Australian cloud lines and the 'Morning Glory.' *Aust. Meteor. Mag.*, **35,** 31–45.

Ono, H., 1975: Algebraic solitary waves in stratified fluids. *J. Phys. Soc. Japan,* **39,** 1082–1091.

Physick, W., 1986: Observations of a solitary wave train at Melbourne, Australia. *Aust. Meteor. Mag.*, **34,** 163–172.

Rottman, J. W., and J. E. Simpson, 1989: The formation of internal bores in the atmosphere: A laboratory model. *Quart. J. Roy. Meteor. Soc.*, **115,** 941–963.

Rotunno, R., J. B. Klemp, and M. L. Weisman, 1988: A theory for strong, long-lived squall lines. *J. Atmos. Sci.*, **45,** 463–485.

Scorer, R. S., 1949: Theory of waves in the lee of a mountain. *Quart. J. Roy. Meteor. Soc.*, **75,** 41–56.

Sha, W., T. Kawamura, and H. Ueda, 1991: A numerical study on sea/land breezes as a gravity current: Kelvin-Helmholtz billows and inland penetration of the sea-breeze front. *J. Atmos. Sci.*, **48,** 1649–1665.

Shreffler, J. H., and F. S. Binkowski, 1981: Observation of pressure jump lines in the Midwest, 10–12 August 1976. *Mon. Wea. Rev.*, **109,** 1713–1725.

Simpson, J. E., 1982: Gravity currents in the laboratory, atmosphere, and ocean. *Ann. Rev. Fluid Mech.*, **14,** 213–234.

——, D. A. Mansfield, and J. R. Milford, 1977: Inland penetration of sea-breeze fronts. *Quart. J. Roy. Meteor. Soc.*, **103,** 47–76.

Smith, R. G., and B. R. Morton, 1984: An observational study of northeasterly 'Morning Glory' wind surges. *Aust. Meteor. Mag.*, **32,** 155–175.

——, 1988: Traveling waves and bores in the lower atmosphere: The 'Morning Glory' and related phenomena. *Earth-Sci. Rev.*, **25,** 267–290.

——, N. Crook, and G. Roff, 1982: The Morning Glory: An extraordinary atmospheric undular bore. *Quart. J. Roy. Meteor. Soc.*, **108,** 937–956.

——, M. J. Coughlan, and J. L. Lopez, 1986: Southerly nocturnal wind surges and bores in northeastern Australia. *Mon. Wea. Rev.*, **114,** 1501–1518.

Tepper, M., 1950: A proposed mechanism of squall lines: The pressure jump line. *J. Meteor.*, **7,** 21–29.

Thorpe, A. J., M. J. Miller, and M. W. Moncrieff, 1982: Two-dimensional convection in non-constant shear: A model of mid-latitude squall lines. *Quart. J. Roy. Meteor. Soc.*, **108,** 739–762.

Tung, K. K., T. F. Chan, and T. Kubota, 1982: Large amplitude internal waves of permanent form. *Stud. Appl. Math.*, **66,** 1–44.

Weisman, M. L., J. B. Klemp, and R. Rotunno, 1988: Structure and evolution of numerically simulated squall lines. *J. Atmos. Sci.*, **45,** 1990–2013.

Wood, I. R., and J. E. Simpson, 1984: Jumps in layered miscible fluids. *J. Fluid Mech.*, **140,** 329–342.